Effects of PMCA and SERCA pump overexpression on the kinetics of cell Ca^{2+} signalling

Marisa Brini[1], Daniele Bano, Sabrina Manni, Rosario Rizzuto[2] and Ernesto Carafoli

Department of Biochemistry and Center for the Study of Biomembranes of the National Research Council (CNR), University of Padova, Viale G. Colombo, 3, 35121 Padova and [2]Department of Experimental and Diagnostic Medicine, Section of General Pathology, University of Ferrara, 44100 Ferrara, Italy

[1]Corresponding author
e-mail: brini@civ.bio.unipd.it

The dynamic interactions of the main pathways for active Ca^{2+} transport have been analysed in living cells by altering the expression of their components. The plasma membrane (PMCA) and the endoplasmic reticulum (ER) (SERCA) Ca^{2+} pumps were transiently overexpressed in CHO cells, and the Ca^{2+} homeostasis in the subcellular compartments was investigated using specifically targeted chimaeras of the Ca^{2+}-sensitive photoprotein aequorin. In resting cells, overexpression of the PMCA and SERCA pumps caused a reduction and an increase in ER [Ca^{2+}] levels, respectively, while no significant differences were detected in cytosolic and mitochondrial [Ca^{2+}]. Upon stimulation with an inositol 1,4,5-trisphosphate (IP$_3$)-generating agonist, the amplitude of the mitochondrial and cytosolic Ca^{2+} rises correlated with the ER [Ca^{2+}] only up to a threshold value, above which the feedback inhibition of the IP$_3$ channel by Ca^{2+} appeared to be limiting.
Keywords: ATPases/calcium homeostasis/photoprotein(s)/pumps/signal transduction

Introduction

In the complex scenario of cellular Ca^{2+} homeostasis, the dynamic equilibrium between its steady-state level and the large swings requested by cell function demands the coordinated operation of Ca^{2+} transporters (pumps, channels, exchangers) and soluble Ca^{2+}-binding proteins (Carafoli, 1987; Petersen *et al*., 1994; Pozzan *et al*., 1994; Clapham, 1995; Berridge, 1997). Major aspects of the operation are its spatio-temporal properties and the role of the involved systems in shaping events such as Ca^{2+} waves, oscillations and localized changes. Their precise and concerted modulation guarantees the fine tuning of Ca^{2+}-dependent cellular activities.

Abundant information is now available on the structure, function and regulation of the individual Ca^{2+}-transporting and -binding proteins. Far less is known on their interplay and their relative contribution to the general process of Ca^{2+} homeostasis within the membranes of cell organelles in living cells. A widely held assumption attributes a housekeeping role to some components [i.e. the plasma membrane Ca^{2+} pump (PMCA)], whereas other components are supposed to react dynamically to larger swings of cell Ca^{2+} [i.e. the SERCA pump, the plasma membrane Na$^+$/Ca^{2+} exchanger, the intracellular channels, e.g. the IP$_3$ and ryanodine (Ry) receptors]. The problem is compounded by inadequate knowledge of the general mechanism by which targeted processes respond to Ca^{2+} changes, i.e. one does not know whether the key point is the availability of total free Ca^{2+} in the cell, or the strictly localized changes produced by the regulated activity of the Ca^{2+} transporting systems. Studies on individual Ca^{2+} controlling systems in intact cells in which Ca^{2+} entry and extrusion occur simultaneously with its binding to soluble proteins and with its organellar sequestration would clearly be helpful. Unfortunately, when transiently overexpressing heterologous proteins, e.g. Ca^{2+} transporters, in cell populations, fluorescent dyes cannot be loaded selectively in the transfected cells (usually ~10–20% of the total). Since the Ca^{2+} signals originate from the entire cell population, the effects of the transfection may be easily overlooked. Single-cell imaging would be an improvement; however, even if positive cells can be identified using a co-transfected reporter (e.g. the green fluorescent protein, GFP), a large statistical analysis is necessary to minimize variability in cell response. We have previously described a successful alternative procedure in which the Ca^{2+}-sensitive photoprotein aequorin is co-transfected with genes of interest (Brini *et al*., 1995). It was thus decided to use it to explore the interplay of the different cellular Ca^{2+} controlling systems. Two commonly used PMCA and SERCA pump isoforms (PMCA4 and SERCA2b) were overexpressed in CHO cells, the effects on the Ca^{2+} concentration in different cell compartments then being monitored with co-expressed targeted aequorin. Cells were studied at rest, upon stimulation with an inositol 1,4,5-trisphosphate (IP$_3$)-generating agonist, and after treatment with the SERCA pump inhibitor 2,5-di-(*tert*-butyl)-1,4-benzohydroquinone (tBuBHQ; Kass *et al*., 1989). Overexpression of the two pumps had distinctive effects on the kinetics of cytosolic and organellar [Ca^{2+}] changes. Interestingly, the perturbation of endoplasmic reticulum (ER) [Ca^{2+}] induced by the overexpression failed to correlate quantitatively with the effects on the cytosol and on the mitochondria, suggesting compensatory and/or controlling mechanisms designed to maintain the changes in Ca^{2+} homeostasis within tolerable borders.

Results

Expression and cellular localization of the Ca^{2+} pumps

In this work, the two main Ca^{2+} removal systems, the PMCA and SERCA pumps (namely the PMCA4 and
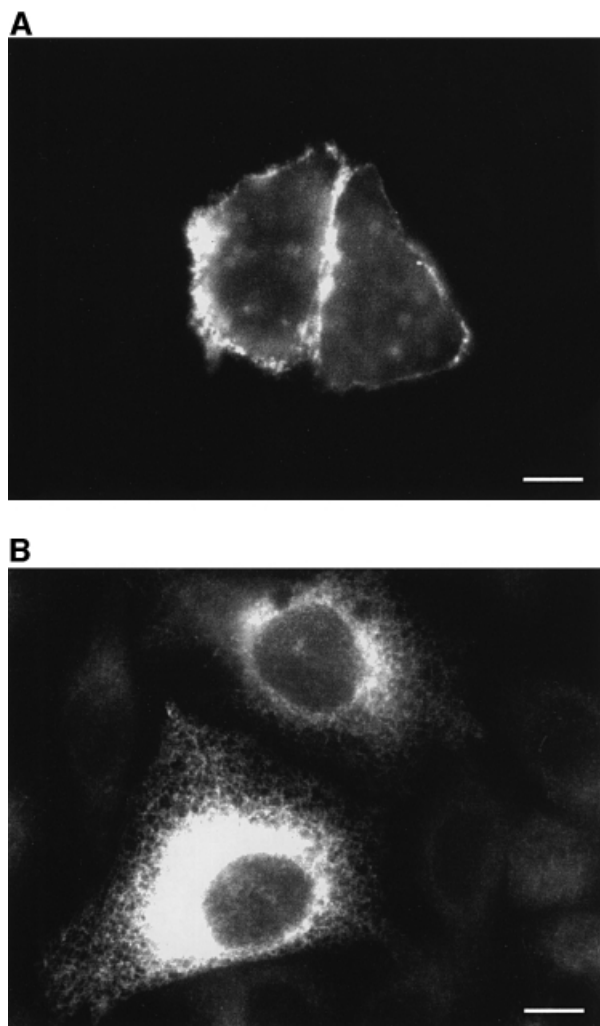
Fig. 1. Immunolocalization of the PMCA (**A**) and SERCA (**B**) pumps in transiently transfected CHO cells. The staining with monoclonal antibodies 5F10 and IID8, respectively, was revealed by a FITC-conjugated antibody. Immunocytochemistry was performed as described in Materials and methods. Bars, 10 μm.

Fig. 2. Western blot analysis of PMCA- and SERCA-overexpressing cells. Lysates from the transiently transfected CHO cells were prepared and separated by SDS–PAGE as described in Materials and methods. Lane 1 corresponds to CHO cells co-transfected with erAEQ/PMCA4 expression plasmids, lane 2 to cells co-transfected with erAEQ/SERCA2b, lane 3 to cells transfected with the empty plasmid and lane 4 to cells transfected with the erAEQ expression vector. The blot was probed with four different monoclonal antibodies: 5F10 (**A**), JA9 (**B**), IID8 (**C**) and 12CA5 (**D**).

SERCA2b isoforms), were transiently overexpressed in CHO cells to 'perturb' Ca²⁺ homeostasis, and the effects on cytosolic, ER and mitochondrial [Ca²⁺] were monitored using co-transfected targeted aequorin chimaeras as specific probes (Rizzuto *et al*., 1992; Brini *et al*., 1995; Montero *et al*., 1995). At first, the correct sorting and the level of overexpression were analysed by immunocytochemistry and western blotting.

The subcellular distribution of the endogenous and overexpressed pumps is illustrated in the representative cells chosen for Figure 1. Figure 1A shows that the newly expressed PMCA pump was correctly targeted to the plasma membrane: antibody 5F10 (which reacts with all isoforms of the pump) yielded a clear signal concentrated at the cell surface. The positive cells were ~25% of the population, but in a fraction of them (~25% of the positive cells) no rim staining was visible, i.e. the overexpressed PMCA was retained in the ER. However, the ER-retained pump was inactive (see below, and E.Carafoli, unpublished observations) and was thus unlikely to influence
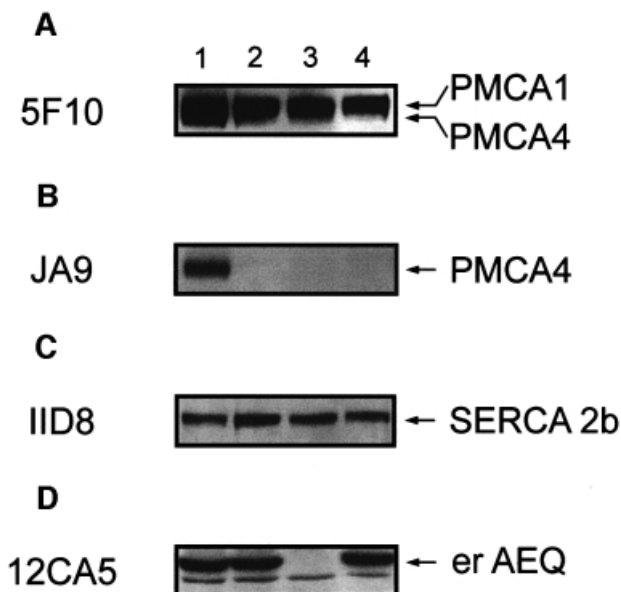
Ca²⁺ homeostasis. The signal from the endogenous PMCA pump was barely above background level. Figure 1B shows that both control cells and cells successfully transfected with the SERCA2 cDNA reacted to the SERCA2 IID8 antibody. The intensity of the signal in control cells was much lower and varied but minimally among cells. As in the case of PMCA, the percentage of transfected cells was ~25%, and the signal revealed the typical staining pattern of ER proteins, i.e. a delicate reticulum distributed throughout the cytoplasm.

The level of overexpression of the two pumps was estimated by western blotting and densitometric analysis (Figure 2). Parallel batches of CHO cells were co-transfected with erAEQ/PMCA4 (lane 1), erAEQ/SERCA2b (lane 2), the empty expression vector (lane 3) or erAEQ (lane 4) (where erAEQ is aequorin targeted to the ER). The same nitrocellulose membrane was probed with four different antibodies. Two were PMCA specific: monoclonal antibody 5F10 and monoclonal antibody JA9 (a kind gift of Dr J.T.Penniston, Rochester, MN), which is specific for the PMCA4 pump. Figure 2A and B shows that in cells transfected with the PMCA4 cDNA both antibodies recognized a protein migrating with the apparent molecular mass of 134 kDa expected of the PMCA4 isoform. That the overexpressed protein was PMCA4 was clearly revealed by antibody JA9 (Figure 2B). Since CHO cells contain both isoforms 1 and 4 of the PMCA pump (the latter only in minimal amounts), antibody 5F10 also reacted with a band of ~135 kDa (corresponding to isoform 1) in all cells, including control cells. Figure 2C shows the immunolabelling of the cells with the anti-SERCA2 antibody IID8. Figure 2D indicates that the level
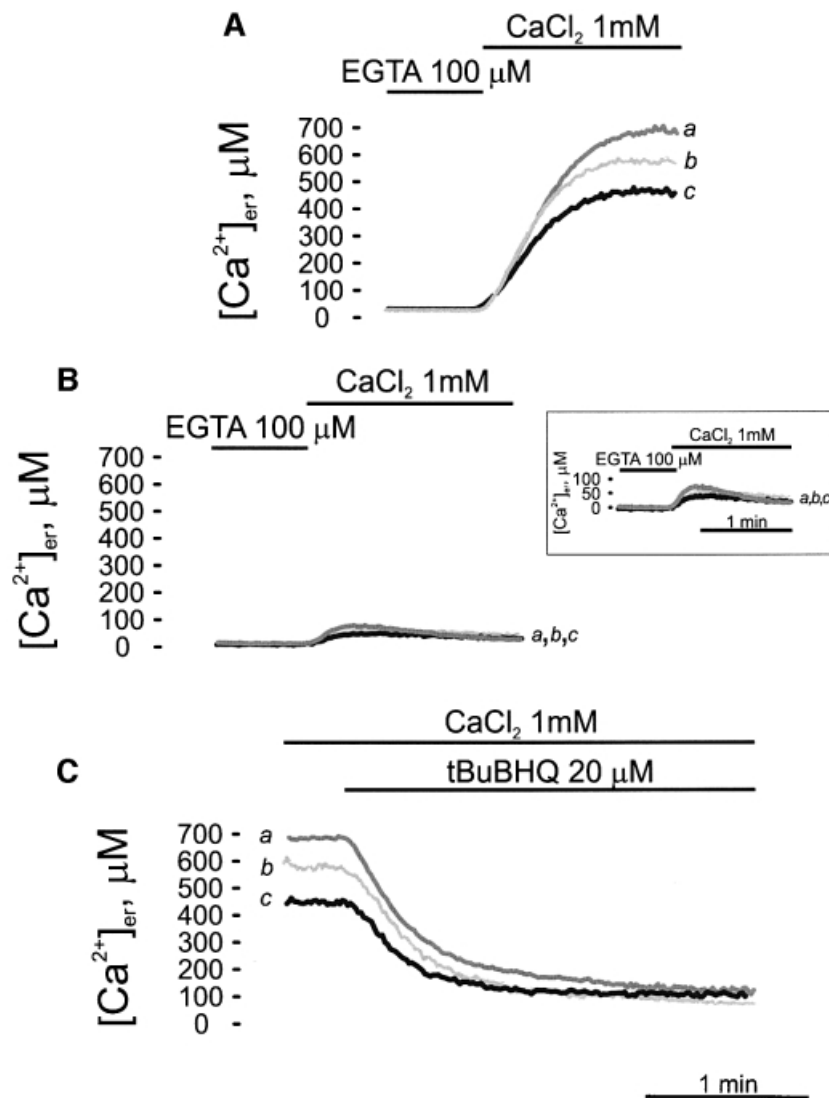
Fig. 3. Kinetics of ER lumen refilling upon re-addition of $CaCl_2$ to Ca^{2+}-depleted cells (**A**) and effects of the Ca^{2+} ATPase inhibitors thapsigargin (TG) (**B**) and tBuBHQ (**C**). The experiments shown in this figure were performed on CHO cells transiently expressing either erAEQ (trace b), erAEQ/PMCA4 (trace c) or erAEQ/SERCA2b (trace a). Transfected CHO cells were depleted of Ca^{2+} as described in Materials and methods and then incubated with 5 µM coelenterazine n in modified KRB supplemented with 600 µM EGTA. After extensive washing, the coverslip with the cells was placed in the thermostatted chamber of the luminometer and perfused with KRB medium supplemented with 100 µM EGTA. Where indicated, the EGTA was replaced with 1 mM $CaCl_2$. In (B) the cells were incubated with TG in the final 5 min of reconstitution. In (C), where indicated, the cells were challenged with 20 µM tBuBHQ. These data and those in the following figures are typical of at least nine independent experiments, which yielded equivalent results. The inset shows the experiment of (B) in an amplified ordinate scale.

of erAEQ expression (revealed by the anti-HA1 epitope tag antibody 12CA5) was similar in the three batches of transfected cells. As expected, no signal was detected in lane 3 (empty vector). The levels of overexpression of PMCA4 (lane 1, Figure 2A) and SERCA2 pumps (lane 2, Figure 2C) in the extracts of the total cell population were estimated at ~50% ($n = 8$) for PMCA4 and ~45% ($n = 6$) for SERCA2b, over the respective controls (lanes 3 and 4). Since the average transfection efficiency approached 25%, the increase of the pump protein in overexpressing cells, corrected for the whole cell population, would correspond to ~200%, i.e. the total amount of pump would be ~3-fold the endogenous level. The overexpression of one pump apparently failed to influence the expression of the other, at variance with what has been reported for stable clones (Guerini *et al*., 1995; Liu *et al*., 1996).

The resting [Ca²⁺] in the ER

erAEQ was used to measure the intralumenal Ca^{2+} concentration, $[Ca^{2+}]_{er}$ (Figure 3). Functional aequorin was reconstituted with a modified prosthetic group, coelenterazine n, in order to decrease the affinity of the photoprotein and thus monitor the high values of $[Ca^{2+}]_{er}$ (Barrero *et al*., 1997).

In all experiments, erAEQ reconstitution was carried out after depleting the ER lumen of Ca^{2+} with 5 µM ionomycin; as shown in previous work, the depletion protocol had no appreciable effect on the morphology and lumenal continuity of the organelle (Montero *et al*., 1995). When Ca^{2+} was added back to the perfusion chamber containing the cells in Ca^{2+}-free Krebs–Ringer buffer (KRB), a major increase in $[Ca^{2+}]_{er}$ was observed. In the experiment shown in Figure 3, parallel batches of CHO

cells, transfected with either erAEQ, erAEQ/PMCA4 or erAEQ/SERCA2b, were perfused with KRB supplemented with 1 mM $CaCl_2$. Cells overexpressing the SERCA pump exhibited a higher steady-state value of $[Ca^{2+}]_{er}$ (trace a; 679.75 ± 81 μM, $n = 16$) than control cells (trace b; 556.46 ± 74 μM, $n = 13$). Interestingly, PMCA-overexpressing cells (trace c) showed a lower plateau value of Ca^{2+} in the ER lumen (451.00 ± 77 μM, $n = 14$) (Figure 3A). The initial kinetics of ER refilling in the experiments of Figure 3A was comparable in the three cell batches; however, differences may have gone undetected since the concentration of Ca^{2+} in the perfused chamber equilibrated in seconds, and cells could have responded asynchronously, affecting the accuracy of the measurements and obscuring possible differences in Ca^{2+} pumping rate. The rate of Ca^{2+} accumulation clearly fell as $[Ca^{2+}]_{er}$ rose, and came to a stop when the store was full (Mogami *et al.*, 1998).

The specific SERCA pump inhibitor thapsigargin (TG) (Thastrup *et al.*, 1990) was used to show that Ca^{2+} accumulation in the ER was due to the SERCA pump (and thus confirming that the ER-retained PMCA pump was inactive in PMCA overexpressers). At the end of the reconstitution step the cells were incubated with 1 μM TG, transferred to the luminometer chamber and perfused with KRB/Ca^{2+}. Under these conditions essentially the same marginal refilling (~10% of that in untreated cells) of the ER lumen occurred in control, SERCA- and PMCA-overexpressing cells (Figure 3B).

Then, the effect of SERCA blockers added after the steady-state level of $[Ca^{2+}]_{er}$ had been attained was investigated. A different SERCA blocker, tBuBHQ, was used, which, unlike TG, can be efficiently delivered through the plastic tubing of the luminometer. Figure 3C shows that tBuBHQ caused the gradual depletion of the ER Ca^{2+} content. The traces show that the kinetics of the leak channel depended on the level of intralumenal free calcium concentration, eventually leading in all cases to the essentially complete depletion of the lumen; lines c and a correspond to PMCA- and SERCA-overexpressing cells, respectively, and line b to control cells.

The effect of agonist stimulation on cytosolic and ER [Ca²⁺]

The differences in the level of free $[Ca^{2+}]$ in the ER lumen observed in Figure 3A could be expected to affect cytosolic Ca^{2+} homeostasis: the reduction in $[Ca^{2+}]_{er}$ should result in reduced Ca^{2+} release from the ER, whereas its increase would lead to augmented Ca^{2+} release. The representative experiment of Figure 4 shows the cytosolic Ca^{2+} concentration ($[Ca^{2+}]_c$) monitored with cytAEQ (where cytAEQ is aequorin targeted to the cytosol), and the $[Ca^{2+}]_{er}$ monitored with erAEQ, in control cells (Figure 4A), and in PMCA- (Figure 4B) and SERCA- (Figure 4C) overexpressing cells. As expected, during the phase of Ca^{2+} release from the stores induced by the IP_3-generating agonist, $[Ca^{2+}]_c$ increased, whereas $[Ca^{2+}]_{er}$ decreased. In the figure, the two traces were superimposed to highlight the time course of the two events, and to emphasize that, after the treatment with the agonist, at the time when $[Ca^{2+}]_c$ peaked the depletion of the ER lumen was still incomplete.
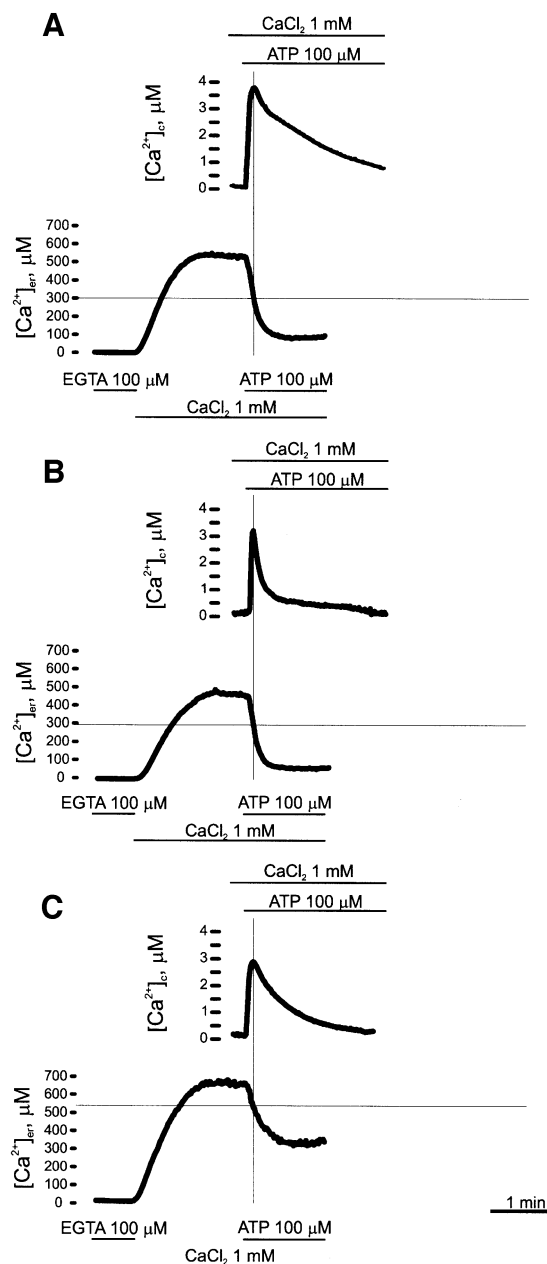

Fig. 4. Effects of the IP_3-generating agonist ATP on $[Ca^{2+}]_c$ and $[Ca^{2+}]_{er}$ in control (**A**), PMCA- (**B**) and SERCA- (**C**) overexpressing CHO cells. The $[Ca^{2+}]$ of the two compartments was monitored in parallel batches of cells co-transfected with either cytAEQ or erAEQ. In the case of erAEQ, Ca^{2+} depletion, aequorin reconstitution and Ca^{2+} refilling were carried out as in Figure 3; after a steady-state $[Ca^{2+}]$ level was reached (as observed in Figure 3), the cells were challenged, where indicated, with 100 μM ATP. In the case of cytAEQ, aequorin reconstitution was carried out by incubating the cells with 5 μM coelenterazine wt as described in Materials and methods. Where indicated, the cells were challenged with 100 μM ATP.

The finding that no differences in the $[Ca^{2+}]_c$ basal values were detected between control cells and cells overexpressing the pumps was unexpected; however, the steep response curve of aequorin makes it difficult to estimate $[Ca^{2+}]$ accurately at concentrations <200–300 nM. Thus, attempts were made to measure the basal $[Ca^{2+}]_c$ with fura-2 by computerized image analysis in cells overexpressing the PMCA and SERCA pumps identified

by co-transfection with the GFP. Unfortunately, the experiment was inconclusive: resting values (i.e. background subtracted 340/380 nm fluorescence values) were similar in control and PMCA- or SERCA-overexpressing cells (six experiments, 146 cells; data not shown). Thus, although the lower steady-state $[Ca^{2+}]_{er}$ is very likely to depend on a reduction in $[Ca^{2+}]_c$ (see Discussion), no direct experimental demonstration of this was obtained.

At variance with resting $[Ca^{2+}]_c$, both the amplitude and the duration of the agonist-dependent increases in $[Ca^{2+}]_c$ were significantly reduced in PMCA- and SERCA-over-expressing cells. The average height of the peaks was 3.12 ± 0.51 µM ($n = 9$) in the former case (Figure 4B), and 2.84 ± 0.46 µM ($n = 9$) in the latter case (Figure 4C), as compared with 3.95 ± 0.43 µM ($n = 9$) for control cells (Figure 4A). While the faster clearance of the cytosolic Ca^{2+} signal could be easily explained by the increased Ca^{2+} pumping activity (see below), the decrease in its peak height suggests decreased release from the ER. This was largely expected in PMCA overexpressers, which have a lower $[Ca^{2+}]_{er}$, but could appear surprising in SERCA overexpressers, which contain higher $[Ca^{2+}]_{er}$. The scenario was clarified by the direct monitoring of $[Ca^{2+}]_{er}$, which revealed major differences in the dynamics of Ca^{2+} release between control cells and PMCA and SERCA overexpressers. Figure 4 shows that a rapid and nearly complete Ca^{2+} release was induced by agonist stimulation in control (Figure 4A) and PMCA-over-expressing (Figure 4B) cells. Conversely, in SERCA overexpressers (Figure 4C) the release rate rapidly slowed down (half decay time of the steady-state plateau phase was 21.5 ± 5.95 s, $n = 6$ as opposed to 7.02 ± 1.71 s, $n = 8$ and 6.29 ± 1.68 s, $n = 9$ for controls and PMCA overexpressers, respectively), most likely due to the Ca^{2+}-dependent inhibition of IP_3-gated channels (see Discussion). As a consequence, $[Ca^{2+}]_{er}$ stabilized at an intermediate plateau level (215 ± 42.5 µM, $n = 12$), also due to the larger Ca^{2+} re-uptake into the ER of SERCA overexpressers.

The overexpression of the PMCA and SERCA pumps had an obvious effect on the Ca^{2+} influx across the plasma membrane elicited by the emptying of intracellular Ca^{2+} stores [the capacitative Ca^{2+} entry (CCE); Clapham, 1995; Putney and McKay, 1999]. In the experiments described here, the contribution of this influx pathway to the $[Ca^{2+}]_c$ rise elicited by the agonist corresponded to the phase of slow decline of the trace after its peak. This long-lasting decay phase was accelerated in both PMCA- and SERCA-overexpressing cells. While the increased activity of the PMCA pump could be expected to offset the capacitative Ca^{2+} influx in the former, in SERCA-overexpressing cells $[Ca^{2+}]_{er}$ was decreased to a level comparable to that of control cells at rest (i.e. ~550 µM) at the peak of $[Ca^{2+}]_c$. Apparently, the capacitative influx mechanism became activated only when a critical threshold of $[Ca^{2+}]_{er}$ was reached, rather than by the variation in the state of ER filling *per se* (see Discussion).

The return of $[Ca^{2+}]_c$ toward basal values, in the continuous presence of agonist, was more efficient in PMCA- than in SERCA-overexpressers and in control cells. The peak value in control and SERCA-overexpressing cells decayed to 50% of its height in 14.37 ± 4.36 s ($n = 8$) and 17.32 ± 3.84 s ($n = 9$), respectively, while the
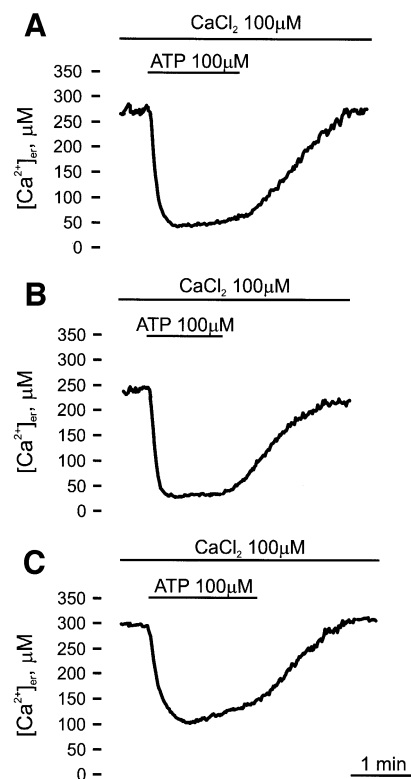

Fig. 5. Refilling of Ca^{2+} stores after agonist stimulation in control (**A**), PMCA- (**B**) and SERCA- (**C**) overexpressing CHO cells. Ca^{2+} depletion, aequorin reconstitution and Ca^{2+} refilling were carried out as in Figure 3, except that KRB was supplemented with 100 µM $CaCl_2$ instead of 1 mM. After a steady-state $[Ca^{2+}]$ level was reached, the cells were challenged, where indicated, with 100 µM ATP.

total time for the return to basal $[Ca^{2+}]$ level was 140.13 ± 43.63 s ($n = 7$) and 94.92 ± 17.80 s ($n = 8$). PMCA-overexpressing cells cleared instead 50% of the cytosolic signal much more rapidly (5.72 ± 1.49 s, $n = 10$) and recovered the resting $[Ca^{2+}]_c$ in 61.65 ± 23 s ($n = 8$). This may have been due to differences in activity (related to localization, i.e. the plasma membrane versus the ER) between the two pumps and/or to the balance between the activity of the pumps and the release or influx channels. Next we evaluated the rate of recovery in conditions where ATP was removed 20 s after its addition and consequently the intracellular release channels were closed: the time of recovery was 58.07 ± 3.19 s ($n = 5$) in control cells, 42.43 ± 2.33 s ($n = 5$) in PMCA-over-expressing cells and 45.01 ± 4.71 s ($n = 5$) in SERCA-overexpressing cells.

Finally, the rate of refilling of the Ca^{2+} stores after agonist stimulation was investigated (Figure 5). In order to reduce aequorin consumption in these long protocols and to maintain a good signal to noise ratio throughout the experiment, $[Ca^{2+}]$ in the KRB was reduced to 100 µM. Under these conditions, a lower state of filling of the ER was attained [241.78 ± 39.16 µM ($n = 11$) in controls (Figure 5A), 210.61 ± 40.56 µM ($n = 13$) in PMCA overexpressers and 272.08 ± 39.52 µM ($n = 13$) in SERCA overexpressers (Figure 5B and C, respectively)]. Upon agonist stimulation, a major decrease in $[Ca^{2+}]_{er}$ was observed, reaching a value of ~58.00 ± 9.06 µM ($n = 12$)
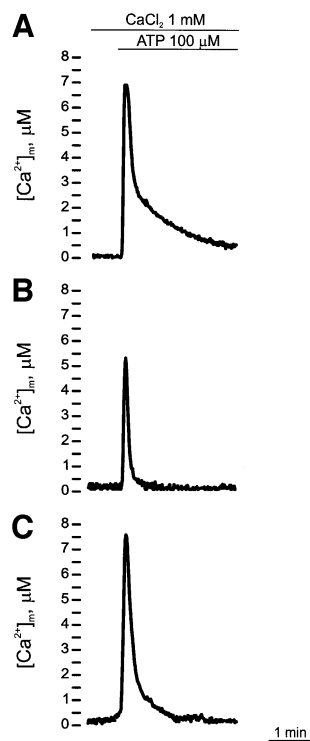
Fig. 6. Effects of ATP on $[Ca^{2+}]_{mt}$ in control (**A**), PMCA- (**B**) and SERCA- (**C**) overexpressing CHO cells, monitored with wt mtAEQ. wt mtAEQ was reconstituted in the same way as cytAEQ (see Materials and methods); where indicated, the cells were challenged with 100 µM ATP.

Fig. 7. Effects of ATP on $[Ca^{2+}]_{mt}$ in control (**A**), PMCA- (**B**) and SERCA- (**C**) overexpressing CHO cells, monitored with mutated mtAEQ. Mutated mtAEQ was reconstituted in the same way as wt mtAEQ (see Materials and methods) and the luminescence signal calibrated in $[Ca^{2+}]$ values according to Montero *et al.* (1995). Where indicated, the cells were challenged with 100 µM ATP.

in control cells. In agreement with the data of Figure 3A, lower and higher values were attained in PMCA- and SERCA-overexpressing cells, respectively. Interestingly, in the continuous presence of the agonist, a significant rate of Ca²⁺ re-uptake (1.33 ± 0.30 µM/s, $n = 10$ versus 0.42 ± 0.14 µM/s, $n = 15$ and 0.46 ± 0.14 µM/s, $n = 11$ in control and PMCA-overexpressing cells, respectively) was observed only in SERCA-overexpressing cells. The washout of the agonist caused a major increase in the rate of Ca²⁺ accumulation and the refilling of the store to the pre-stimulatory values. In agreement with the results of Figure 3A, no difference in the maximal rate of refilling was observed between control, PMCA- and SERCA-overexpressing cells: 2.83 ± 0.99 µM/s ($n = 15$) for control cells, 2.70 ± 0.53 µM/s ($n = 13$) for PMCA-overexpressing cells and 2.51 ± 1.16 µM/s ($n = 13$) for SERCA-overexpressing cells.

Mitochondrial Ca²⁺
Next, experiments were performed to explore whether the alterations in the level of ER filling affected mitochondrial Ca²⁺ concentration, $[Ca^{2+}]_m$. Previous work had shown that large changes of $[Ca^{2+}]_m$ occurred upon stimulation of cells with specific agonists (Rizzuto *et al.*, 1994; Hajnoczky *et al.*, 1995), and evidence had been provided for the existence of microdomains of high $[Ca^{2+}]_c$ produced by the agonists in close proximity to mitochondria (Rizzuto *et al.*, 1993; Csordas *et al.*, 1999): close contacts between mitochondria and the ER have been detected in HeLa cells (Rizzuto *et al.*, 1998). Since a direct relationship was demonstrated between the $[Ca^{2+}]_m$ rise
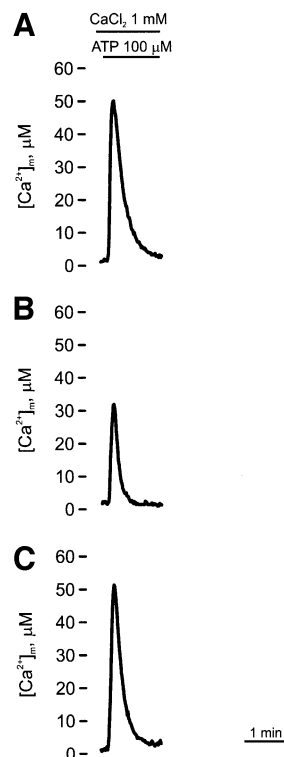
and the increase in NADH (Hajnoczky *et al.*, 1995) and ATP (Jouaville *et al.*, 1999) levels, the size of the generated microdomains could directly modulate the energetic metabolism of the cell.

The experiments presented in Figures 6 and 7 show the effects of the alteration of $[Ca^{2+}]_{er}$ produced by the overexpression of the pumps on $[Ca^{2+}]_m$. In the experiment of Figure 6, cells were transiently transfected with mitochondrial aequorin (mtAEQ) (Figure 6A), mtAEQ/PMCA4 (Figure 6B) or mtAEQ/SERCA2b (Figure 6C). As expected, the stimulation with ATP induced a large, transient increase in $[Ca^{2+}]_m$ in control cells (Figure 6A) (peak value 7.03 ± 1.82 µM, $n = 11$). In PMCA4-overexpressing cells (Figure 6B) the height of the peak was significantly lower (5.42 ± 1.73 µM, $n = 14$), whereas in cells overexpressing the SERCA2b pump (Figure 6C) its height was instead slightly higher (peak value 7.42 ± 1.32 µM, $n = 14$). Somewhat surprisingly, these results only partially matched those on the $[Ca^{2+}]_{er}$ and $[Ca^{2+}]_c$: in keeping with the concept of localized microdomains of high $[Ca^{2+}]$ at the mouth of the IP₃-modulated channels that are sensed by neighbouring mitochondria one would have expected the mitochondrial Ca²⁺ signal to reflect the differences in ER Ca²⁺ filling.

Since mitochondrial wild-type (wt) aequorin would be completely saturated at high $[Ca^{2+}]$ values, $[Ca^{2+}]_m$ measurements were performed with a variant of mtAEQ having reduced Ca²⁺ affinity (Montero *et al.*, 2000) and thus adequate to measure $[Ca^{2+}]$ values >10 µM (Figure 7). The experiments with this mtAEQ revealed that the

height of the $[Ca^{2+}]_m$ peak induced by ATP was 33.32 ± 10.60 µM ($n = 11$) in PMCA-overexpressing cells (Figure 7B) and 52.21 ± 16.61 µM ($n = 17$) in control cells (Figure 7A); these data essentially matched the differences seen with the wild-type aequorin. The height of the peak in SERCA-overexpressing cells (Figure 7C) was very similar to that of the controls: 53.57 ± 16.58 µM ($n = 14$), in agreement with the result with wt mtAEQ.

The agonist-dependent increase in $[Ca^{2+}]_m$ would be expected to increase the activity of the mitochondrial Ca^{2+} release antiporters, which extrude Ca^{2+} in exchange for Na^+ (or H^+) and thus return $[Ca^{2+}]_m$ to basal values after stimulation. Moreover, the Ca^{2+} buffering and the dissipation of the microdomains also participate in the recovery of resting $[Ca^{2+}]_m$. The rate of mitochondrial Ca^{2+} efflux was different in control cells (half decay of the peak in 11.04 ± 3.60 s, $n = 11$) with respect to cells overexpressing the PMCA pump (half decay of the peak in 5.00 ± 1.55 s, $n = 15$). In cells overexpressing the SERCA pump the half decay of the peak approached that of the controls (9.09 ± 2.00 s, $n = 16$). However, a difference became evident when the total time required for the return to the basal $[Ca^{2+}]$ level, as opposed to the half decay time, was monitored: 106.90 ± 31.04 s ($n = 7$) in control cells versus 64.17 ± 20.18 s ($n = 7$) in SERCA-overexpressing cells.

Discussion

The cytosol uses the strategic placement and the dynamic properties of Ca^{2+} transporters and channels to generate spatially and temporally complex Ca^{2+} fluctuations, which modulate a number of cellular functions (Lee *et al.*, 1997; Wilson *et al.*, 1998; Kasai, 1999). The lumen of the ER, which is itself heterogeneous (Meldolesi and Pozzan, 1998), may use a similar strategy to translate complex Ca^{2+} signals. High amplitude Ca^{2+} signals must by necessity be transient to avoid Ca^{2+} cytotoxicity: indications have been provided that their duration, i.e. their termination, may be controlled by specific characteristics of the IP_3/Ry receptors, which replenish the cytosol with Ca^{2+}, and by the rate of Ca^{2+} removal from the cytosol. The latter involves both Ca^{2+} extrusion across the plasma membrane by the PMCA pump and, especially, ER Ca^{2+} re-uptake (Camello *et al.*, 1996). Additional control mechanisms may operate at the lumenal side of the ER membrane (Favre *et al.*, 1996; Mogami *et al.*, 1998), i.e. a feedback inhibition of the Ca^{2+} uptake reaction by the magnitude of the ER Ca^{2+} load.

The biochemical properties of the systems (i.e. the proteins) participating in cellular Ca^{2+} homeostasis are reasonably well known, but their relative contribution to the restoration of the pre-stimulus conditions is not. A key factor is the difficulty of studying their integrated function in the living cell; no matter how useful, analyses on membrane preparations have inherent limitations, related to the absence of native regulators [i.e. calmodulin, G proteins, phospholamban, etc.; see Guerini and Carafoli (1999) for a review of the topic] and to the practical impossibility of reproducing the exact physiological microenvironment. This work has tried to overcome these restrictions by altering the relative amounts of the two high affinity Ca^{2+}-removing systems, the PMCA and SERCA pumps, and by monitoring the effects of the alteration on the cytoplasmic and organellar Ca^{2+}.

Some of the results described in this work are of particular interest. One was the finding that the steady-state level of $[Ca^{2+}]_{er}$ was affected in opposite ways by the overexpression of the two pumps (reaching values that were 22% higher than in control cells for SERCA overexpressers and 20% lower for PMCA overexpressers). While the former result was not surprising, the latter was less obvious. A simple explanation for it would have been the compensatory decreased expression of the SERCA pump, as observed in stably transfected clones (Liu *et al.*, 1996). This possibility, which was unlikely in transient expressions, was ruled out by the quantification of SERCA and PMCA protein levels (Figure 2C). A more likely explanation would be the decrease in SERCA activity linked to the lowering of $[Ca^{2+}]_c$, induced by the increased Ca^{2+} extrusion by the overexpressed PMCA. The decrease of $[Ca^{2+}]_c$ could not be documented, but reasonable explanations could be offered for this negative result: (i) intrinsic limitations in the methodology (e.g. the steep response curve of aequorin impairs the monitoring of $[Ca^{2+}]$ <100–200 nM, while the high variability among cells in the imaging experiments could have masked minor differences between controls and transfected cells); and (ii) the $[Ca^{2+}]_c$ reduction could have been confined to local domains and would have gone undetected in bulk $[Ca^{2+}]_c$ measurements: very small changes, which the methodology used here would have missed, could still have been effective (see e.g. Camello *et al.*, 1996).

The amplitude and the kinetics of the agonist-dependent $[Ca^{2+}]_c$ rise are also worth a comment. Perhaps unexpectedly, the Ca^{2+} re-uptake by the ER was not the most effective mechanism for terminating the cytosolic Ca^{2+} signals (at least in CHO cells): in PMCA-overexpressing cells the clearance of the $[Ca^{2+}]_c$ transient was much more effective in the continuous presence of the agonist. If the agonist was rapidly washed away, the resting $[Ca^{2+}]_c$ level was recovered in similar times. This finding was most probably related to the different locations of the two pumps. Whereas during the agonist-dependent opening phase of the IP_3 receptor the activity of the SERCA pump was likely to become short-circuited by that of the Ca^{2+} release channel, the PMCA pump, whose essential task under resting conditions is that of extruding Ca^{2+} penetrating from the extracellular medium, would rapidly increase the rate of Ca^{2+} ejection as soon as the ER Ca^{2+} channels open and some of the released Ca^{2+} trickles over to the cytosol at large (see Camello *et al.*, 1996).

The slow decline of the $[Ca^{2+}]_c$ transient after the agonist-induced peak evidently was the algebraic sum of two opposite components: the Ca^{2+} removal from the cytosol (into the ER or the extracellular medium) and its entry from the external space by the CCE. The latter process was also inhibited by the overexpression of the pumps. However, the mechanism of CCE inhibition is likely to be different in the two cases. In SERCA-overexpressing cells, the slower influx through the plasma membrane channels most likely depended on the maintenance of a higher $[Ca^{2+}]_{er}$ value after stimulation with the IP_3-generating agonist (see Hofer *et al.*, 1998). In PMCA-overexpressing cells, it is very likely that the

inhibition was due to the increased extrusion of incoming Ca^{2+} through the overexpressed PMCA pump. Possibly, the extrusion efficiency could even be increased by microdomains of high [Ca^{2+}] generated in the sub-plasma membrane region (Marsault *et al*., 1997).

The reduction in the height of the [Ca^{2+}]$_c$ peak observed with both pumps was expected in the case of the PMCA pump, since the lower [Ca^{2+}]$_{er}$ induced by its over-expression (see above) would slow down the efflux rate from the ER. On the other hand, the higher [Ca^{2+}]$_{er}$ in SERCA-overexpressing cells was likely to have reduced the peak [Ca^{2+}]$_c$ height due to a rapid feedback inhibition of the IP$_3$ receptor (and/or to the re-uptake in the ER). This suggestion was supported by the bell-shaped calcium response curve of the IP$_3$ receptor (Bezprozvanny *et al*., 1991) and was confirmed by the incomplete ER emptying in SERCA-overexpressing cells shown in Figure 4C.

As to mitochondria, the amplitude of the agonist-dependent [Ca^{2+}]$_m$ rise in SERCA-overexpressing cells was similar to that of controls, in spite of the much lower [Ca^{2+}]$_c$ rise. This apparently surprising result can be explained as follows. The low affinity of the Ca^{2+} uniporter renders the mitochondrial Ca^{2+} uptake dependent on the [Ca^{2+}] hotspots generated at the ER–mitochondrial contacts by the opening of the IP$_3$ receptor. Thus, if the hotspots were enhanced by the higher [Ca^{2+}]$_{er}$, they would compensate for the reduced release of Ca^{2+} from the ER leaving the mitochondrial Ca^{2+} transient virtually un-affected. Conversely, in PMCA-overexpressing cells, the [Ca^{2+}]$_{er}$ levels (i.e. the [Ca^{2+}] hotspots) and the rise in global [Ca^{2+}]$_c$ were diminished, significantly reducing the [Ca^{2+}]$_m$ increase with respect to the controls.

The return of [Ca^{2+}]$_m$ to the basal level was faster in cells overexpressing the pumps. This is likely to have been related to [Ca^{2+}]$_c$. The extrusion of Ca^{2+} from mitochondria during the decline phase of [Ca^{2+}]$_m$ is normally counteracted by its uptake, which depends on the long-lasting elevation of [Ca^{2+}]$_c$ due to Ca^{2+} influx. The sharp reduction of the influx process in PMCA- and SERCA-overexpressing cells (see Figure 6) will shift the balance between uptake and release toward extrusion, thus allow-ing a faster return of [Ca^{2+}]$_m$ to the basal values.

The correlation between the changes of [Ca^{2+}]$_{er}$ and [Ca^{2+}]$_m$ allows one final observation on ER Ca^{2+} buffering. A comparison of Figures 4 and 6 shows that while the height of the agonist-induced [Ca^{2+}]$_m$ peak was the same in cells overexpressing the SERCA pump and the controls, the decrease in [Ca^{2+}]$_{er}$ was markedly reduced in the former case. At first glance, the two sets of data may seem to be inconsistent. However, the inconsistency would disappear if one also considers the Ca^{2+} buffering capacity of the Ca^{2+}-binding proteins in the ER, of which calreticulin is the most abundant. Calreticulin contains a highly acidic C-terminal domain capable of binding 25 Ca^{2+} ions per molecule with low affinity ($K_D \sim 2$ mM). The central portion of the protein contains instead a high affinity Ca^{2+}-binding site, which modulates the activity of the SERCA pump (Camacho and Lechleiter, 1995; John *et al*., 1998). Conversely, the increase in [Ca^{2+}]$_{er}$ in cells overexpressing the SERCA pump would activate the low affinity sites in calreticulin, increasing its Ca^{2+} buffering capacity, and eventually allowing a large Ca^{2+} release for a comparatively small [Ca^{2+}]$_{er}$ decrease.

In conclusion, the modification of the molecular reper-toire for active Ca^{2+} transport in living cells has revealed a scenario that only partially matched the predictions from the known biochemical properties of the Ca^{2+} pumps. It was striking to find that the general pattern of Ca^{2+} homeostasis was preserved in the face of glaring alter-ations in Ca^{2+} handling by the intracellular compartments. Evidently, even if both pumps are individually necessary for Ca^{2+} homeostasis [as revealed for instance by the deleterious consequences of their genetic defects (Odermatt *et al*., 1996; Street *et al*., 1998; Sakuntabhai *et al*., 1999)], a fine, and essential, dynamic interplay between them must be at work in cells. Perhaps the distribution, the amount and the relative ratio of the two pumps in different cellular types could change in response to specific functional requirements, to optimally fulfil the demands for the fine tuning of the intracellular Ca^{2+} effects.

Materials and methods

Cell culture and transfection
CHO cells were grown in Ham's F12 medium, supplemented with 10% fetal calf serum (FCS), in 75 cm^2 Falcon flasks; before transfection, they were seeded onto 13 or 24 mm glass coverslips (for aequorin and fura-2 measurements) or on 24-multiwell plates (for western blot analysis) and allowed to grow to 50% confluence. At this stage, transfection with 3 µg of plasmid DNA (or 1.5:1.5 µg in the case of co-transfection) was carried out as previously described (Rizzuto *et al*., 1995). Aequorin, fura-2 measurements, immunocytochemistry and western blot analysis were then performed 36 h later.

Immunolocalization
Thirty-six hours after transfection, CHO cells were processed for immunofluorescence as follows: they were fixed with 3.7% formaldehyde in phosphate-buffered saline (PBS; 140 mM NaCl, 2 mM KCl, 1.5 mM KH$_2$PO$_4$, 8 mM Na$_2$HPO$_4$ pH 7.4) for 20 min, washed three times with PBS and then incubated for 10 min in PBS supplemented with 50 mM NH$_4$Cl. Permeabilization of membranes was obtained with a 5 min incubation with 0.1% Triton X-100 in PBS, followed by a 1 h wash with 1% gelatin (type IV, from calf skin) in PBS. Cells were then incubated for 1 h at 37°C in a wet chamber with monoclonal antibody 5F10 (Affinity Bioreagents Inc., Golden, CO), which recognizes all PMCA isoforms at a 1:100 dilution in PBS, or with the same dilution of monoclonal antibody IID8 (Affinity Bioreagents), which recognizes the SERCA2 isoform. Staining was then carried out with fluorescein isothiocyanate (FITC)-labelled anti-mouse secondary antibodies (1:50 dilution in PBS; Dako, Glostrup, Denmark). After each incubation, cells were washed four times with PBS. Fluorescence was then analysed with an Olympus IMT-2 microscope equipped with a 12-bit digital cooled camera (Micromax-1300Y; Princeton Instruments Inc., Trenton, NJ). Images were acquired using Metamorph software (Universal Imaging Corporation, West Chester, PA).

Western blot analysis
The protein samples (cell lysates) were separated on 10% polyacrylamide gels and transferred to nitrocellulose membranes. Two hundred micrograms of total protein were loaded onto each lane. The sheet was stripped and reprobed several times with antibody 5F10, monoclonal antibody JA9 (a kind gift of Dr J.T.Penniston, Rochester, MN), which only recognizes the PMCA4 isoform, antibody IID8, which recognizes the SERCA2 isoforms, or antibody 12CA5 (Roche Diagnostic, Milan, Italy), which recognizes the HA1 tag added to the aequorin chimaeras (Field *et al*., 1988). After incubation with anti-mouse horseradish peroxidase-conjugated secondary antibodies (Santa Cruz Biotechnology, Santa Cruz, CA) the blot was developed with ECL reagents (Amersham Life Science, Buckinghamshire, UK). The quantitative analysis was carried out by densitometric analysis using the IPLab gel program (Signal Analytics Corporation, Vienna, VA).

Aequorin measurements

As discussed in Results, the Ca^{2+} content of the ER had to be drastically reduced before the reconstitution of functional erAEQ. To this end the cells were incubated for 1 h at 4°C in KRB (125 mM NaCl, 5 mM KCl, 1 mM Na_3PO_4, 1 mM $MgSO_4$, 5.5 mM glucose, 20 mM HEPES pH 7.4, 37°C) supplemented with 5 μM coelenterazine n, the Ca^{2+} ionophore ionomycin (5 μM) and 600 μM EGTA. After this incubation, the cells were washed extensively with KRB supplemented with 2% bovine serum albumin and 1 mM EGTA, and transferred to the chamber of a purpose-built luminometer.

Transfected cytAEQ and mtAEQ (wt and mutated) were reconstituted by incubating the cells for 1–3 h with 5 μM coelenterazine wt in Dulbecco's modified Eagle's medium supplemented with 1% FCS, at 37°C in a 5% CO_2 atmosphere.

The additions to the KRB medium (1 mM or 100 μM $CaCl_2$, 100 μM ATP, 20 μM tBuBHQ) were made as specified in the figure legends. The experiments were terminated by lysing the cells with 100 μM digitonin in a hypotonic Ca^{2+}-rich solution (10 mM $CaCl_2$ in H_2O) to discharge the remaining aequorin pool. The light signal was collected and calibrated into $[Ca^{2+}]$ values as previously described (Brini *et al.*, 1995; Montero *et al.*, 1995; Rizzuto *et al.*, 1995; Barrero *et al.*, 1997). In brief, a 13 mm round coverslip with the transfected cells was placed in a perfused, thermostatted chamber placed in close proximity to a low-noise photomultiplier, with a built-in amplifier discriminator. The output of the discriminator was captured by a Thorn-EMI photon counting board and stored in an IBM-compatible computer for further analyses. The aequorin luminescence data were calibrated off-line into $[Ca^{2+}]$ values, using a computer algorithm based on the Ca^{2+} response curve of wt and mutant aequorins, as previously described (Brini *et al.*, 1995; Montero *et al.*, 1995).

Fura-2 measurements

Fura-2 loading was performed as previously described (Malgaroli *et al.*, 1987). The coverslip was placed in a thermostatted (37°C) chamber on the stage of an inverted fluorescence microscope (Zeiss Axiovert 100TV) connected to a cooled charge coupled device (CCD) camera (Micromax-800PB; Princeton Instruments, Inc.). The sample was illuminated alternately at 340/380 nm and the emitted light (filtered with an interference filter centred at 510 nm) was collected by the camera. Images were acquired using Metafluor software (Universal Imaging Corporation). The ratio values (1 ratio image/s) were calculated off-line, after background subtraction from each single image.

Acknowledgements

References

Barrero,M.J., Montero,M. and Alvarez,J. (1997) Dynamics of $[Ca^{2+}]$ in the endoplasmic reticulum and cytoplasm of intact HeLa cells: a comparative study. *J. Biol. Chem.*, **272**, 27694–27699.

Berridge,M.J. (1997) Elementary and global aspects of calcium signalling. *J. Physiol.*, **499**, 291–306.

Bezprozvanny,I., Watras,J. and Ehrlich,B.E. (1991) Bell-shaped calcium-response curves of $Ins(1,4,5)P_3$ and calcium-gated channels from endoplasmic reticulum of cerebellum. *Nature*, **351**, 751–754.

Brini,M., Marsault,R., Bastianutto,C., Alvarez,J., Pozzan,T. and Rizzuto,R. (1995) Transfected aequorin in the measurement of cytosolic Ca^{2+} concentration $([Ca^{2+}]_c)$: a critical evaluation. *J. Biol. Chem.*, **270**, 9896–9903.

Camacho,P. and Lechleiter,J.D. (1995) Calreticulin inhibits repetitive calcium waves. *Cell*, **82**, 765–771.

Camello,P., Gardner,J., Petersen,O.H. and Tepikin,A.V. (1996) Calcium dependence of calcium extrusion and calcium uptake in mouse pancreatic acinar cells. *J. Physiol.*, **490**, 585–593.

Carafoli,E. (1987) Intracellular calcium homeostasis. *Annu. Rev. Biochem.*, **56**, 395–433

Clapham,D.E. (1995) Calcium signaling. *Cell*, **80**, 256–268.

Csordas,G., Thomas,A.P. and Hajnoczky,G. (1999) Quasi-synaptic calcium signal transmission between endoplasmic reticulum and mitochondria. *EMBO J.*, **18**, 96–108.

Favre,C.J., Schrenzel,J., Jacquet,J., Lew,D.P. and Krause,K.-H. (1996) Highly supralinear feedback inhibition of Ca^{2+} uptake by the Ca^{2+} load of intracellular stores. *J. Biol. Chem.*, **271**, 14925–14930.

Field,J., Nikawa,J., Broeck,D., MacDonald,B., Rodgers,L., Wilson,I.A., Lerner,R.A. and Wigler,M. (1988) Purification of a RAS-responsive adenyl-cyclase complex from *Saccharomyces cerevisiae* by use of an epitope addition method. *Mol. Cell. Biol.*, **8**, 2159–2165.

Guerini,D. and Carafoli,E. (1999) The calcium pumps. In Carafoli,E. and Klee,C.B. (eds), *Calcium as a Cellular Regulator*. Oxford University Press, Oxford, UK, pp. 249–278.

Guerini,D., Schröder,S., Foletti,D. and Carafoli,E. (1995) Isolation and characterization of a stable Chinese hamster ovary cell line overexpressing the plasma membrane calcium pump. *J. Biol. Chem.*, **270**, 14643–14650.

Hajnoczky,G., Robb-Gaspers,L.D., Seitz,M.B. and Thomas,A.P. (1995) Decoding of cytosolic calcium oscillations in the mitochondria. *Cell*, **82**, 415–424.

Hofer,A.M., Fasolato,C. and Pozzan,T. (1998) Capacitative Ca^{2+} entry is closely linked to the filling state of internal Ca^{2+} stores: a study using simultaneous measurements of I_{CRAC} and intraluminal $[Ca^{2+}]$. *J. Cell Biol.*, **140**, 325–334.

John,L.M., Lechleiter,J.D. and Camacho,P. (1998) Differential modulation of SERCA2 isoforms by calreticulin. *J. Cell Biol.*, **142**, 963–973.

Jouaville,L.S., Pinton,P., Bastianutto,C., Rutter,G.A. and Rizzuto,R. (1999) Regulation of mitochondrial ATP synthesis by calcium: evidence for a long-term metabolic priming. *Proc. Natl Acad. Sci. USA*, **96**, 13807–13812.

Kasai,H. (1999) Comparative biology of Ca^{2+}-dependent exocytosis: implications of kinetic diversity for secretory function. *Trends Neurosci.*, **22**, 88–93.

Kass,G.E.N., Duddy,S.K., Moore,G.A. and Orrenius,S.A. (1989) 2,5-Di(*tert*-butyl)-1,4-benzohydroquinone rapidly elevates cytosolic Ca^{2+} concentration by mobilizing the inositol 1,4,5-trisphosphate-sensitive Ca^{2+} pool. *J. Biol. Chem.*, **264**, 15192–15198.

Lee,M.G., Xu,X., Zeng,W., Diaz,J., Kuo,T.H., Wuytack,F., Raeymaekers,L. and Muallem,S. (1997) Polarized expression of Ca^{2+} pumps in pancreatic and salivary gland cells. *J. Biol. Chem.*, **272**, 15771–15776.

Liu,B.F., Xu,X., Fridman,R., Muallem,S. and Kuo,T.H. (1996) Consequences of functional expression of the plasma membrane Ca^{2+} pump isoform 1a. *J. Biol. Chem.*, **271**, 5536–5544.

Malgaroli,A., Milani,D., Meldolesi,J. and Pozzan,T. (1987) Fura-2 measurements of cytosolic free Ca^{2+} in monolayers and suspensions of various types of animal cells. *J. Cell Biol.*, **105**, 2145–2155.

Marsault,R., Murgia,M., Pozzan,T. and Rizzuto,R. (1997) Domains of high Ca^{2+} beneath the plasma membrane of living A7r5 cells. *EMBO J.*, **16**, 1575–1581.

Meldolesi,J. and Pozzan,T. (1998) The heterogeneity of ER Ca^{2+} stores has a key role in nonmuscle cell signaling and function. *J. Cell Biol.*, **142**, 1395–1398.

Mogami,H., Tepikin,A.V. and Petersen,O.H. (1998) Termination of cytosolic Ca^{2+} signals: Ca^{2+} reuptake into intracellular stores is regulated by the free Ca^{2+} concentration in the store lumen. *EMBO J.*, **17**, 435–442.

Montero,M., Brini,M., Marsault,R., Alvarez,J., Sitia,R., Pozzan,T. and Rizzuto,R. (1995) Monitoring dynamic changes in free Ca^{2+} concentration in the endoplasmic reticulum of intact cells. *EMBO J.*, **14**, 5467–5475.

Montero,M., Alonso,M.T., Carnicero,E., Cuchillo-Ibanez,I., Albillos,A., Garcia,A.C., Garcia-Sancho,J. and Alvarez,J. (2000) Chromaffin-cell stimulation triggers fast millimolar mitochondrial Ca^{2+} transients that modulate secretion. *Nature Cell Biol.*, **2**, 57–61.

Odermatt,A., Taschner,P.E.M., Khanna,V.K., Busch,H.F.M., Karpati,G., Jablecki,C.K., Breuning,M.H. and MacLennan,D.H. (1996) Mutations in the gene encoding SERCA1, the fast-twitch skeletal muscle sarcoplasmic reticulum Ca^{2+} ATPase, are associated with Brody disease. *Nature Genet.*, **14**, 191–194.

Petersen,O.H., Petersen,C.C.H. and Kasai,H. (1994) Calcium and hormone action. *Annu. Rev. Physiol.*, **56**, 297–319.

Pozzan,T., Rizzuto,R., Volpe,P. and Meldolesi,J. (1994) Molecular and cellular physiology of intracellular Ca^{2+} stores. *Physiol. Rev.*, **74**, 595–636.

Putney,J.W.J. and McKay,R.R. (1999) Capacitative calcium entry channels. *BioEssays*, **21**, 38–46.

Rizzuto,R., Simpson,A.W.M., Brini,M. and Pozzan,T. (1992) Rapid changes of mitochondrial Ca²⁺ revealed by specifically targeted recombinant aequorin. *Nature*, **358**, 325–328.

Rizzuto,R., Brini,M., Murgia,M. and Pozzan,T. (1993) Microdomains of cytosolic Ca²⁺ concentration sensed by strategically located mitochondria. *Science*, **262**, 744–747.

Rizzuto,R., Bastianutto,C., Brini,M., Murgia,M. and Pozzan,T. (1994) Mitochondrial Ca²⁺ homeostasis in intact cells. *J. Cell Biol.*, **126**, 1183–1194.

Rizzuto,R., Brini,M., Bastianutto,C., Marsault,R. and Pozzan,T. (1995) Photoprotein mediated measurement of [Ca²⁺] in mitochondria of living cells. *Methods Enzymol.*, **260**, 417–428.

Rizzuto,R., Pinton,P., Carrington,W., Fay,F.S., Fogarty,K.E., Lifshitz, L.M., Tuft,R.A. and Pozzan,T. (1998) Close contacts with the endoplasmic reticulum as determinants of mitochondrial Ca²⁺ responses. *Science*, **280**, 1763–1766.

Sakuntabhai,A. *et al*. (1999) Mutations in ATP2A2, encoding a Ca²⁺ pump, cause Darier disease. *Nature Genet.*, **21**, 271–277.

Street,V.A., McKee-Johnson,J.W., Fonseca,R.C., Tempel,B.L. and Nobel-Trauth,K. (1998) Mutations in a plasma membrane Ca²⁺ ATPase gene cause deafness in deafwaddler mice. *Nature Genet.*, **19**, 390–394.

Thastrup,O., Cullen,P.J., Drobak,B.J., Hanley,M.R. and Dawson,A.P. (1990) Thapsigargin, a tumor promoter, discharges intracellular Ca²⁺ stores by specific inhibition of the endoplasmic reticulum Ca²⁺-ATPase. *Proc. Natl Acad. Sci. USA*, **87**, 2466–2470.

Wilson,B.S., Pfeiffer,J.R., Smith,A.J., Oliver,J.M., Oberdorf,J.A. and Wojcikiewicz,R.J.H. (1998) Calcium-dependent clustering of inositol 1,4,5-trisphosphate receptors. *Mol. Biol. Cell*, **9**, 1465–1478.